Article published online: 2022-08-16

Original Article

Role of Three-dimensional Printing in Neurosurgery: An Institutional Experience

Ankit Chaudhary, Sanjeev Chopra, Virendra Deo Sinha

Department of Neurosurgery, Sawai Man Singh Medical College, Jaipur, Rajasthan, India

Abstract

Background: Recent advancements in three-dimensional (3D) printing technology in the field of neurosurgery have given a newer modality of management for patients. In this article, we intend to share our institutional experience regarding the use of 3D printing in three modalities, namely, cranioplasty using customized 3D-printed molds of polymethylmethacrylate, 3D-printed model-assisted management of craniovertebral (CV) junction abnormalities, and 3D model-assisted management of brain tumors. **Materials and Methods:** A total of 55 patients were included in our study between March 2017 and December 2019 at S. M. S Medical College, Jaipur, India. 3D-printed models were prepared for cranioplasty in 30 cases, CV junction anomalies in 18 cases, and brain tumors in 7 cases. Preoperative and postoperative data were analyzed as per the diagnosis. **Results:** In cranioplasty, cranial contour and approximation of the margins were excellent and esthetic appearance improved in all patients. In CV junction anomalies, neck pain and myelopathy were improved in all patients, as analyzed using the visual analog scale and the Japanese Orthopedic Association Scale score, respectively. Our questionnaire survey revealed that 3D models for brain tumors were useful in understanding space interval and depth intraoperatively with added advantage of patient education. **Conclusion:** Rapid prototyping 3D-printing technologies provide a practical and anatomically accurate means to produce patient-specific and disease-specific models. These models allow for surgical planning, training, simulation, and devices for the assessment and treatment of neurosurgical disease. Expansion of this technology in neurosurgery will serve practitioners, trainees, and patients.

Keywords: *Cranioplasty, craniovertebral junction, customized, neurosurgery*

Introduction

Three-dimensional (3D) printing has revolutionized the practice of rapid prototyping since its initial emergence in the 1980s. This technique has enabled the fabrication of physical, 3D models from computeraided designs through additive manufacturing, in which successive layers of material are deposited onto underlying layers to construct 3D objects.[1] Using this type of manufacturing, traditional intermediary stages of product development including tooling, supply chains, and production lines are eliminated, allowing concepts to be quickly and inexpensively translated into both prototypes and products. Several methods of printing have been developed that leverage unique material properties to selectively cure or fix specific areas on an individual layer. Most notably, fused deposition modeling utilizes a thermoplastic material that hardens after being heated during extrusion, whereas stereolithography (SLA) employs a low-power ultraviolet laser to solidify a liquid photosensitive polymer. Within the last decade, applications for 3D printing technology have expanded greatly in the manufacturing industry as a result of numerous innovations that have markedly reduced production and technology costs, improved the level of accuracy of printed objects, and increased the range of printable materials. Applications within clinical medicine are also emerging due to 3D printing's ability to produce individualized models, devices, and implants that can potentially improve patient care. The field of neurosurgery, in particular, has experienced substantial progress as a result of the usage of 3D printing because most of the surgical procedures and corresponding pathology that neurosurgeons encounter involve

How to cite this article: Chaudhary A, Chopra S, Sinha VD. Role of three-dimensional printing in neurosurgery: An institutional experience. Asian J Neurosurg 2021;16:531-8.

Submitted: 19-Oct-2020 **Revised:** 01-Feb-2021
Accepted: 16-Mar-2021 **Published:** 14-Sep-2021

Address for correspondence:
Dr. Sanjeev Chopra, Department of Neurosurgery, Sawai Man Singh Medical College, Jaipur, Rajasthan, India.
E-mail: choprasanjeevdr@gmail.com

Access this article online

Website: www.asianjns.org

DOI: 10.4103/ajns.AJNS_475_20

Quick Response Code:

intricate, minute anatomical structures that cannot be outwardly observed; neuroimaging has become an integral component of clinical practice.[2] This technology has enabled structures to be noninvasively visualized for both diagnosis and surgical treatment; however, most imaging methods including X-ray, computed tomography (CT), and magnetic resonance imaging (MRI) acquire images in either 2D or a 3D volume in 2D slices.[3] Therefore, appreciation of the 3D relationships between these structures within a limited surgical aperture is often difficult. 3D printing could provide a practical solution to this issue. With this technology, anatomical structures can be reconstructed from 3D volumes and subsequently fabricated as physical models, which can then be used for surgical planning and education for both patients and trainees. Similarly, the capabilities of 3D printing can be applied to the design of surgical simulations. Simulations provide a realistic representation of the surgical procedure without the risk of potential harm to a patient. 3D printing has enabled the production of customizable, high-resolution simulators that can create a realistic, immersive training environment.[4] 3D printing in neurosurgery has focused upon three main areas: the creation of patient-specific anatomical models for surgical planning, training, and education; the design of neurosurgical devices for the assessment and treatment of neurosurgical diseases; and the development of biological tissue-engineered implants. In this article, we discuss the institutional experience of 3D printing in three modalities of neurosurgery, namely, cranioplasty, craniovertebral (CV) junction anomalies, and brain tumors.

Materials and Methods

Cranioplasty

Thirty patients who underwent customized cranioplasty using 3D-printed mold with PMMA casting over it were studied prospectively. Institutional review board approval and patient or caregiver consent for photographs were obtained before the initiation of the study. Patients were evaluated with multislice helical CT scan with slice thickness of 0.8 mm. Digital Imaging and Communications in Medicine (DICOM) data were processed and converted to 3D images with MIMICS 13.1 Software (Interactive Medical Image Control System; Materialise Inc., Leuven, Belgium) [Figure 1].

Image of implant mold was generated by a digital subtraction mirror-imaging process whereby the normal side of the cranium was used as a model. Smoothing technique by the MIMICS 13.1 Software was used to process stair-like surface of the 3D-implant model. The pre- and postcraniectomy CT images were merged, and the 3D implant images were then cropped. Prefabrication of the mold was performed by fused depositional modeling of the polylactic acid beads. The design process typically lasts between 4 and 5 h, and the 3D mold printing lasts on an average 10 h and the mold was then plasma sterilized. Under GA, after aseptic draping, all the patients reexplored.

Figure 1: Three-dimensional CT reconstructed image of a 26-year-old male patient with left FTP craniectomy defect

Scalp tissue was carefully dissected, temporalis muscle was sharply dissected of the dura mater to expose the sphenoidal edge of the skull defect. The PMMA implant was constructed using the prefabricated mold during the dissection procedure. To prevent adhesion between the implant and the mold, surface of the mold was covered with bone wax or even saline may be used. The PMMA resin was prepared by mixing polymer powder with a liquid monomer. PMMA resin was evenly distributed onto inner half of the prefabricated mold and then compressed with the external half. Minor trimming around the margins with the microdrill was done to achieve exact fit into the defect. The PMMA implant was fixed to the defective region with titanium self-tapping screws. Table 1 shows the clinical summary of the patients enrolled for Cranioplasty. CT scan with 3D reconstruction was done postoperatively to analyze implant contour and margin apposition [Figure 2].

Craniovertebral junction anomalies

In total, 18 patients with complex CV junction abnormalities were enrolled in the study, including one patient who was known to have chronic myeloid leukemia with AAD and basilar invagination (BI). All patients were examined using digital X-rays and dynamic CT of the CV junction, CT angiography of the neck vessels, and MRI of the CV junction and cervical spine. 3D-assisted models of the CV junction along with vertebral artery (VA) were developed for all 18 patients, and CT angiographic images of these patients were used to extract the 3D file in surface tessellation language (STL) format. This STL file was sent to a 3D printer station for printing the model. The models were prepared using acrylonitrile butadiene styrene polymer by a fused deposition modeling printer.

This model provided detailed knowledge of the bony and vascular anatomy. Bony abnormalities such as occipitalized atlas, os odontoideum, bifid arch, and block vertebrae could be studied better using these models. More importantly,

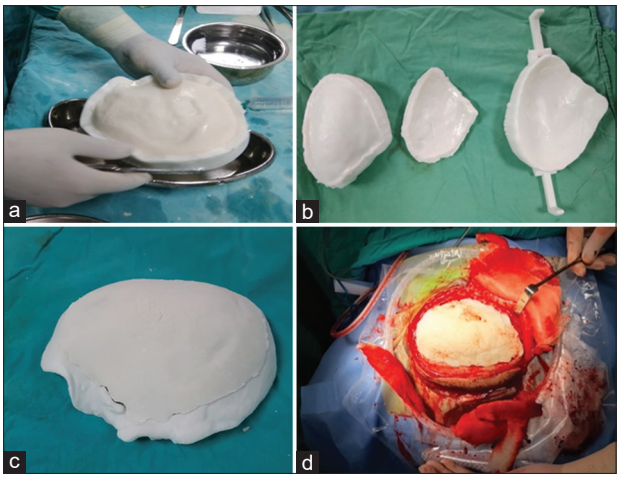

Figure 2: PMMA resin even spread over inner half of the mold. (a) PMMA implant shown in the center with the inner and outer half of the mold. (b) PMMA customized prosthesis assembled over cranial defect printout to ensure exact margin apposition. (c) Placement of PMMA customized prosthesis over the cranial defect Intraoperatively (d)

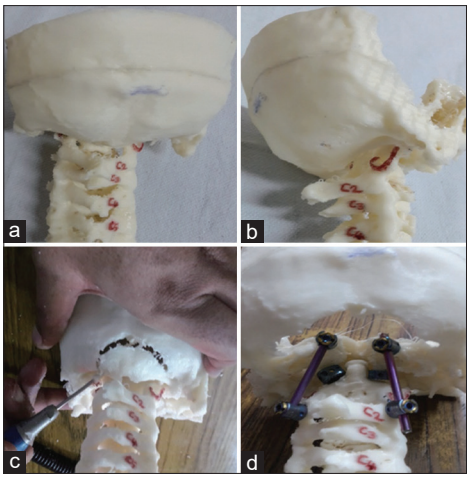

Figure 3: Basiocciput with cv junction along with subaxial cervical vertebrae (a) A three-dimensional-printed model of a patient with occipitalized atlas. (b) Lateral view of the model. (c) Practice using the model. (d) Model with occiput–C2 screws.

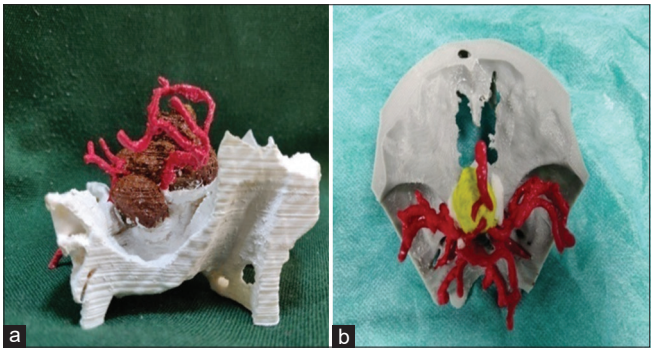

Figure 4: (a) Three-dimensional model of recurrent suprasellar tumor (b) Three-dimensional model of planum sphenoid meningioma

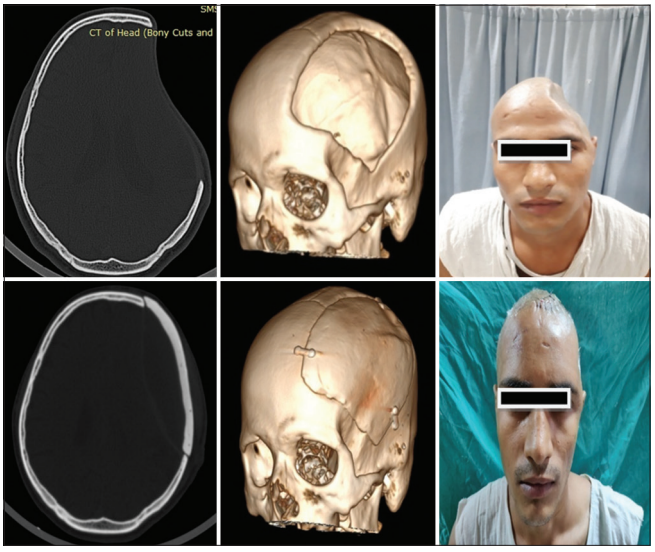

Figure 5: The first row showing preoperative images of a patient with left FTP craniectomy defect. The second row showing corresponding postoperative images with excellent restoration of margins and cranial contour

the VA course could be exactly delineated using the model. The surgical procedure was rehearsed on the model before the surgery. Figure 3 shows the 3D model of craniovertebral junction and practice performed on 3D model. The preoperative clinical features and improvement in symptoms were assessed using the Japanese Orthopedic Association score (JOA score). Radiological improvement was assessed by comparing the preoperative and postoperative craniometric indices: the atlantodental interval, Chamberlain's line, and Wackenheims clivus canal line. Dynamic flexion–extension radiographs were used to confirm the presence of irreducibility, defined as nonalignment of C1–C2 (determined on lateral CV junction radiography) after extension (neck movement) or application of cervical traction (for 48 h). Crutchfield cervical traction was applied, starting with 7%–8% of body weight (2–5 kg depending on age and weight) in extension. The head of the bed was elevated to provide countertraction. The weight was increased every 4 h by 0.5–1 kg, to a maximum of 12%–13% of body weight. Patients were operated using the principle of neural decompression with stabilization of the CV junction complex. All patients in this study underwent posterior fixation with or without C1–C2 joint realignment; the operative strategy was based on whether a reducible or an irreducible dislocation was present. One patient with a reducible dislocation was treated using C1–C2 transarticular screw fixation, first described by Magerl and Seemann in 1987.[5] Occipitocervical fixation first described by Olerud *et al*.[6] was performed in ten patients. C1–C2 fixation was performed in the remaining seven patients, as first described by Goel and Laheri[7] and later modified by Harms and Melcher,[8] who used a rod instead of a plate to connect the C1–C2 screws. In cases where the C2 pedicles were not accessible, C2 translaminar screws were inserted. C1–C2 joint realignment with a spacer or bone graft insertion and reduction of AAD and BI using the "compression, extension, and reduction" sequence, as described by Salunke *et al*.[9] and Chandra *et al*.,[10]

respectively, were performed in 11 patients. Follow-up clinical and radiological evaluations were performed between 2 and 10 months postoperatively, and preoperative and postoperative JOA scores were compared. The total JOA score was used to assess motor and sensory functions of the four extremities and the sphincter, which amounted to a total of 17 points [Table 2]. Follow-up X-ray and CT of the neck were performed to investigate fusion maturation and bone growth at 1–3 months, defined as bone trabeculae between the C1–C2 facets without the presence of any gap. Cystic lucencies around the implants or along the endplates and linear defects within the bridging trabeculae suggested nonfusion. Table 3 shows summary of patients with cv junction anomalies and their preoperative and postoperative comparisons.

Brain tumors

The patients' imaging data were acquired preoperatively by various modalities, such as CT, MRI, and CT angiography. Informed consent was obtained from the patients with respect to the creation of 3D–lesion models using a 3D printer. We have created 3D computer graphics models consisting of all structures required. DICOM data were processed on image analysis software. First, we extracted the region of interest, separated it from the other structures, and removed noise data. Subsequently, we transformed SLA (STL) data to make a 3D model from the voxel data of DICOM. While the extracted areas from the voxel data hold an appropriate data volume and accuracy, are converted into STL format that is a general-purpose output format for the 3D models, as triangular polygon mesh by surface image-rendering technique automatically. The coordinates of the extracted data from various imaging techniques were adjusted manually on the reconstructed virtual multidirectional planes to fit in the individual anatomical structure. Finally, we made each 3D model data written in the binary STL format with different color codes for tumor tissue and related structures shown in figure 4. Evaluation

Table 1: Clinical summary of patients

Case No.	Age (yrs)/sex	Diagnosis	Location	Side	Pre op GCS	Post op GCS	Operation Time (min)	Complication
1	25/m	TBI	FTP	Right	15	15	130	None
2	35/m	TBI	FTP	Right	15	15	145	Post op CT s/o frontal and parietal contusion
3	55/m	TBI	FTP	Left	15	15	155	Uneven contour
4	25/f	TBI	FTP	Left	7	10	180	None
5	24/m	TBI	FTP	Left	15	15	135	None
6	23/m	TBI	FTP	Left	15	15	190	None
7	32/m	TBI	FT	Bilateral	15	15	170	Post op ct s/o, B/l ED hematoma, infection with wound dehiscence at 13 months
8	26/m	TBI	FTP	Right	15	15	165	None
9	34/m	TBI	FTP	Left	15	15	145	None
10	26/m	TBI	FTP	Left	15	15	150	None
11	24/m	TBI	FTP	Left	15	15	155	None
12	13/m	INFARCTION	FTP	Right	11	12	140	None
13	28/m	TBI	FTP	Right	15	15	160	None
14	21/m	TBI	FTP	Right	15	15	165	Uneven contour
15	50/f	TBI	FTP	Left	15	15	130	None
16	24/m	TBI	FTP	Right	3	4	135	None
17	35/f	TBI	FTP	Left	8	8	165	None
18	45/f	TBI	FTP	Right	15	15	152	None
19	38/m	TBI	Frontal	R > L	15	15	140	None
20	12/m	TBI	FP	Left	15	15	144	None
21	38/m	TBI	FTP	Right	13	13	155	None
22	52/m	TBI	FTP	Left	15	15	142	None
23	45/f	TBI	FTP	Right	9	9	151	None
24	52/m	TBI	FTP	Left	13	13	138	None
25	59/m	TBI	FTP	Right	11	11	152	None
26	39/m	TBI	FTP	Left	15	15	148	None
27	48/f	TBI	FTP	Left	10	10	158	None
28	52/m	TBI	FTP	Right	15	15	150	None
29	63/m	TBI	FTP	Left	15	15	156	None
30	58/f	TBI	FTP	Left	15	15	148	None

DOA – Date of admission; GCS – Glasgow Coma Scale, TBI – Traumatic brain injury; FTP – Frontal temporal parietal; M – Male; F – Female; ED – Extradural

Table 2: Japanese Orthopedic Association Scale score

Scale for clinical evaluation of myelopathy (0-17 points)	Points
I. Motor function of the upper limb	
Impossible to eat with cutlery or to button shirt	0
Possible to eat with cutlery, impossible to button shirt	1
Possible to button shirt, with great difficulty	2
Possible to button shirt, with difficulty	3
Normal	4
II. Motor function of the lower limb	
Impossible to walk	0
Needs cane or assistance on flat surface	1
Needs assistance on stairs	2
Walks unaided, but slowly	3
Normal	4
III. Sensory function	
Upper limb	
Apparent sensory disorder	0
Minimal sensory disorder	1
Normal	2
Lower limb	
Apparent sensory disorder	0
Minimal sensory disorder	1
Normal	2
Trunk	
Apparent sensory disorder	0
Minimal sensory disorder	1
Normal	2
IV. Bladder function	
Urinary retention or incontinence	0
Sensation of retention, loss of slight flow	1
Urinary retention and/or increase in urinary frequency	2
Normal	3

of 3D model was analysed using a questionnaire survey from operating surgeon.Replace this sentence. We asked the attending physician and chief surgeon to answer a 10-stage evaluation and to provide an explanation on the usefulness of the 3D model. Each surgeon compared the findings using virtual simulation and 3D models with actual surgical findings and objectively evaluated their accuracy and usefulness. Their utility in ascertaining the structure during surgery was evaluated in individual patients as follows: the evaluation was "10" if the virtual simulation and 3D models were useful for accomplishing surgery and for providing important information that is difficult to ascertain using 2D images. The evaluation was "5" if the 3D models provided enough information that could enhance surgical confidence. The evaluation was "0" if the surgeon found that 3D models might be misleading or confusing with respect to the surgery. Scores in between given figures of 0, 5, and 10 were purely based on surgeons' personal interpretation.

Craniovertebral junction anomalies

Among the 18 patients in the study, 10 were male and 8 were female. The mean age of the patients was 24.7 years (range, 7–55 years). One patient had posttraumatic AAD, while the remaining 17 had congenital AAD. Anteroposterior dislocation with or without BI was observed in 16 patients and Arnold Chiari malformation with BI was observed in two patients. Neck pain was the chief presenting complaint in 17 (94.4%) patients. Preoperative and postoperative pain was graded according to the visual analog scale Graded according to visual analogue scale as shown in Table 4. Improvement in pain was categorized as mild (1–2 score), moderate (3–5), or extensive (>5). Neck pain was present in 17 (94.4%) patients, restricted neck movements were seen in 14 (77.7%) patients, progressive weakness of all four limbs was present in 16 (88.8%) patients, and sensory dysfunction was seen in 7 (38.3%) patients. Urinary incontinence/retention was present in 6 (33.3%) patients, and dysphagia/hoarseness of voice was present in 5 (27.7%) patients. Irreducible AAD was seen in 12 (66.66%) patients. Bony abnormalities were noted in 12 patients, including occipitalization of the atlas vertebrae in 5 (27.77%) patients, os odontoideum in 4 (22.22%) patients, and block vertebrae in 3 (16.66%) patients. Anomalous VAs were seen in 7 (38.8%) patients. Occipitocervical fusion was performed in 10 (55.55%) patients, whereas C1–C2 fixation was performed in 8 (44.44%) patients.

Clinical improvement

Fifteen patients showed clinical improvement as evident from the assessment of their JOA scores. Fusion was achieved in 15 patients at the follow-up.

Radiological improvement

Increased atlantodental interval, when present, could be corrected in all patients as observed in the immediate postoperative scans, except for one patient in whom it increased from its preoperative state; however, there was no deterioration in the clinical profile of the patient. BI could be corrected in all patients when present. Figure 5 compares the preoperative and postoperative radiological and patient images.

Brain tumors

3D resin models were created for 7 patients with different diagnoses for preoperative planning and simulation. Surgery was performed in all 7 patients. The characteristics of the patients, tumor pathologies, and surgical approach of the subjects with questionnaire results are shown in Table 5.

Anatomical orientation is difficult to understand, especially when the positional structure relations between the tumor and vital organs are complicated. Various attempts to simulate operative approach with individual patients for anatomical structural confirmation have been performed. Our questionnaire survey on the 3D models revealed several opinions, indicating that a 3D model is useful for surgical support and preoperative simulation in tumor

Table 3: Summary of patients with craniovertebral junction anomalies

Age (year)/sex	Procedure Executed	ADI (mm)			CL (mm)			WCCL (mm)		
		Preoperative	Postoperative	Dt	Preoperative	Postoperative	Dt	Preoperative	Postoperative	Dt
23/female	C1 lateral mass and C2 pedicle screw and rod fixation	4.5	1.4	3.1	+7.3	+5.1	2.2	3.6	−1.5	5.1
50/male	Sub occiput and C2-C3 fixation with foramen magnum decompression by removal of posterior arch of C1	3.4	4.4	−1.0	+6.6	+3.8	2.8	8.6	5.2	3.4
32/male	C1 lateral mass and C2 pedicle screws and rod fixation with C1-C2 spacer placement	5.1	3.8	1.3	+10.6	+6.3	4.3	+6.6	+0.2	6.4
20/male	Reduction of AAD and BI with occipital plate and C2 pedicle screw and rod fixation	5.4	5.2	0.2	+12.9	+11.4	1.5	+3.3	+3.0	0.3
40/female	Reduction of AAD with C1-C2 trans articular fixation	8.4	7.2	1.2	+7.4	+5.2	2.2	+8.9	+7.6	2.3
12/female	Foramen magnum decompression with removal of posterior arch of C1 with C2 pedicle and occipital screw and rod fixation	4.2	3.1	1.1	+7.5	+7.0	0.5	+3.5	−2.9	6.4
7/male	C1 C2 lateral mass pedicle screw and rod fixation with C1-C2 bone graft placement and distraction of joint with removal of posterior arch of C1	8.7	6.7	2.0	−9.9	−15.8	5.9	+12.3	−2.8	15.1
55/male	C1 lateral mass and C2 pedicle screw and rod fixation with C1 C2 joint fusion with bone	4.4	3.2	1.2	−12.4	−13.6	1.2	−8.2	−8.8	0.6
18/female	Foramen magnum decompression with removal of occipitalized C1 posterior arch with cord decompression with C2 trans laminar screw and occipital plate and rod fixation	7.5	5.4	2.1	+9.9	+3.1	6.8	+9.1	−1.8	10.9
20/female	C1-C2 spacer placement with C1 lateral mass and C2 translaminar screw and rod placement	6.3	3.0	3.7	−2.8	−5.6	2.8	−2.4	−11.2	8.8
11/male	Occipital plate with C2 lateral mass screw and rod fixation with C1 C2 fusion using autologous bone	6.9	5.4	1.5	+10.2	+3.9	6.3	+12.0	+5.6	6.4
8/female	Occiput-C2 fixation using rod and screw with bilateral spacer at C1-C2 joint with foramen magnum decompression	7.2	6.5	0.7	−3.6	−11.5	7.9	−6.0	−14.4	8.4
33/male	C1 posterior arch decompression with C1-C2 spacer insertion with sub occiput and C2 pedicle screw and rod fixation	2.2	1.9	0.3	+21.2	+15.3	5.9	−4.9	−4.6	0.3
26/female	Bilateral C1-C2 fixation using C1 lateral mass and C2 translaminar screw and rod placement	8.5	8.3	0.2	−12.2	−14.4	2.3	−5.1	−12.6	7.5
46/male	Foramen magnum decompression with decompression and debulking Cerebellar tonsils with augmented duroplasty with occiput and C3-C4 fixation using plate screw and rod	1.9	1.8	0.1	+18.5	+9.7	8.8+	+10.0	+9.6	0.4
19/female	Reduction of AAD and BI with C1-C2 spacer and occipital plate and C2 translaminar screw and screw and rod fixation	7.1	5.1	2.0	+10.2	+6.2	4.0	+8.6	+3.4	2.2
14/male	C1 lateral mass and C2 left pedicle, right pars screws and rods fixation with placement of spacer into right C1-C2 joint	5.8	2.1	3.7	+4.4	+0.4	4.0	−1.2	−4.6	3.4
11/male	Occipital C2 fusion with right C2 pedicle screw and left C2 laminar screw with rod fixation with C1-C2 distraction and autologous bone placement between C1-C2	4.3	3.9	0.4	+7.9	+6.4	1.5	+10.2	+2.4	7.8

+ – Above line; − – Below line; ADI – Atlanto dental interval; CL – Distance between odontoid tip and chamberlain line; WCCL – Distance between Odontoid tip and Wackenheims line; Dt – Distraction achieved; AAD – Atlantoaxial dislocation; BI – Basilar invagination

Table 4: Visual analog scale

Visual analog scale score improvement	*n* (%)
1-2 (mild)	2 (13.3)
3-5 (moderate)	10 (66.6)
>5 (extensive)	3 (20.0)

Table 5: Questionnaire score of Brain tumour's 3D printed model

Age (year)/sex	Diagnosis	Procedure Executed	Utility evaluation score (out of 10) (based on surgeon)			
			Tumor Size	Tumor figure	Tumor location	Overall
50/male	Recurrent pituitary Macroadenoma	Right pterional Craniotomy with subtotal excision of tumor	8	10	10	9.3
39/female	Right planum sphenoidal Meningioma	Right pterional Craniotomy with gross total excision of tumor	10	10	10	10
25/female	Right cerebellopontine Angle epidermoid	Right retromastoid Suboccipital craniotomy with gross total excision of tumor	10	8	10	9.3
39/male	Left cerebellopontine Angle acoustic schwannoma	Left retromastoid Suboccipital craniotomy with gross total excision of tumor	8	8	5	7
26/female	Pituitary Macroadenoma	Endoscopic transnasal Transsphenoidal gross total excision of tumor	10	10	10	10
55/male	Left frontal lobe Tumor (glioma)	Left frontal craniotomy with gross total excision of tumor	8	8	10	8.6
30/male	Left cerebellopontine Angle acoustic schwannoma	Left retromastoid Suboccipital craniotomy with gross total excision of tumor	8	8	8	8

removal. Although complications may still exist, 3D models for preoperative simulation are useful. Furthermore, 3D models could be useful in understanding space interval and depth through easy visualization and feel. In addition, medical students, comedical staff, and patients who are unfamiliar with the anatomy of the pathology could easily understand the condition with 3D models. Furthermore, the life-size 3D models not only allow observation but also actual cutting and drilling using surgical instruments, which, in turn, could considerably enhance a surgeon's skill and improve risk management for complex surgical procedures.

Discussion

Since 2012, simulation of surgery using life-size 3D models of individual patient's medical images created by 3D printer has been introduced for clinical use, training, and planning of the operative strategy and used in several clinical cases in the literature. Tam *et al*. reported that a 3D model is useful for anatomical understanding of the lesion and helps plan surgical management.[11] In addition, Oishi *et al*. reported on a 3D-printed plaster model for the simulation of neurosurgical operation.[12] Currently, 3D models using individual patient's medical images have been used in other fields; their use has expanded. In the field of forensic medicine, a 3D model is useful to understand the extent of the damage to the victim. For the judiciary officials and jurors, considering that they are not medical professionals, 3D models could be particularly effective in understanding the extent of the injury of the victim. Furthermore, the usefulness of 3D models in the field of clinical medicine has been evaluated; preoperative simulation using 3D models with the da Vinci operation, laparoscopic operation, or transplantation surgery is performed in urologic or pediatric surgery. Surgical simulation utilizing 3D models of disorders, such as cleft lip and palate or funnel chest, is performed in plastic surgery.[13,14] In otolaryngology, 3D models are used in training young doctors to perform petrous bone resection.[15] However, in neurosurgical preoperative simulations, the 3D model technique remains in the experimental prototype stage.

Conclusion

Rapid prototyping 3D-printing technologies provide a practical and anatomically accurate means to produce patient- and disease-specific models. These models allow for surgical planning, training and simulation, and devices for the assessment and treatment of neurosurgical disease. Expansion of this technology in neurosurgery will serve practitioners, trainees, and patients.

Declaration of patient consent

The authors certify that they have obtained all appropriate patient consent forms. In the form the patient(s) has/have given his/her/their consent for his/her/their images and

other clinical information to be reported in the journal. The patients understand that their names and initials will not be published and due efforts will be made to conceal their identity, but anonymity cannot be guaranteed.

Financial support and sponsorship

Nil.

Conflicts of interest

There are no conflicts of interest.

References

1. Liew Y, Beveridge E, Demetriades AK, Hughes MA. 3D printing of patient-specific anatomy: A tool to improve patient consent and enhance imaging interpretation by trainees. Br J Neurosurg 2015;29:712-4.
2. Klein GT, Lu Y, Wang MY. 3D printing and neurosurgery – Ready for prime time? World Neurosurg 2013;80:233-5.
3. Xu WH, Liu J, Li ML, Sun ZY, Chen J, Wu JH. 3D printing of intracranial artery stenosis based on the source images of magnetic resonance angiograph. Ann Transl Med 2014;2:74.
4. Tai BL, Rooney D, Stephenson F, Liao PS, Sagher O, Shih AJ, *et al*. Development of a 3D-printed external ventricular drain placement simulator: Technical note. J Neurosurg 2015;123:1-7.
5. Magerl F, Seemann PS. Stable posterior fusion of the atlas and axis by transarticular screw fixation. In: Kehr P, Weider A, editors. Cervical Spine I. Wien: Springer-Verlag; 1987. p. 322-7.
6. Olerud C, Larsson BE, Rodriguez M. Subaxial cervical spine subluxation in rheumatoid arthritis: A retrospective analysis of 16 operated patients after 1-5 years. Acta Orthop Scand 1997;68:109-15.
7. Goel A, Laheri V. Plate and screw fixation for atlanto-axial subluxation. Acta Neurochir (Wien) 1994;129:47-53.
8. Harms J, Melcher RP. Posterior C1-C2 fusion with polyaxial screw and rod fixation. Spine (Phila Pa 1976) 2001;26:2467-71.
9. Salunke P, Sahoo SK, Deepak AN, Ghuman MS, Khandelwal NK. Comprehensive drilling of the C1-2 facets to achieve direct posterior reduction in irreducible atlantoaxial dislocation. J Neurosurg Spine 2015;23:294-302.
10. Chandra PS, Kumar A, Chauhan A, Ansari A, Mishra NK, Sharma BS. Distraction, compression, and extension reduction of basilar invagination and atlantoaxial dislocation: A novel pilot technique. Neurosurgery 2013;72:1040-53.
11. Tam MD, Laycock SD, Bell D, Chojnowski A. 3-D printout of a DICOM file to aid surgical planning in a 6-year-old patient with a large scapular osteochondroma complicating congenital diaphyseal aclasia. J Radiol Case Rep 2012;6:31-7.
12. Oishi M, Fukuda M, Yajima N, Yoshida K, Takahashi M, Hiraishi T, *et al*. Interactive presurgical simulation applying advanced 3D imaging and modeling techniques for skull base and deep tumors. J Neurosurg 2013;119:94-105.
13. Choi JW, Kim N. Clinical application of three-dimensional printing technology incraniofacial plastic surgery. Arch Plast Surg 2015;42:267-77.
14. Lioufas PA, Quayle MR, Leong JC, McMenamin PG. 3D printed models of cleft palate pathology for surgical education. Plast Reconstr Surg Glob Open 2016;4:e1029.
15. Rose AS, Webster CE, Harrysson OL, Formeister EJ, Rawal RB, Iseli CE. Preoperative simulation of pediatric mastoid surgery with 3D-printed temporal bone models. Int J Pediatr Otorhinolaryngol 2015;79:740-4.